Sliding mode collision-free navigation for quadrotors using monocular vision

— Source link ↗

D. A. Mercado, Pedro Castillo, Rogelio Lozano

Institutions: Rutgers University, University of Technology of Compiègne

Related papers:

- Autonomous navigation and teleoperation of unmanned aerial vehicles using monocular vision

- Quadrotor's trajectory tracking control using monocular vision navigation

- Autonomous flight and obstacle avoidance of a quadrotor by monocular SLAM

- Quadrotors Trajectory Tracking Control with Inaccurate GPS Measurements

- Collision avoidance for quadrotor using stereo vision depth maps

Sliding mode collision-free navigation for quadrotors using monocular vision

Diego Mercado, Pedro Castillo Garcia, Rogelio Lozano

Sliding Mode Collision-Free Navigation for Quadrotors using Monocular Vision

D. A. Mercado[1], P. Castillo[1] and R. Lozano[1,2]

Abstract

Safe and accurate navigation for either autonomous navigation or haptic teleoperation of quadrotors is presented in this article. A second order Sliding Mode (2-SM) control algorithm is used to track desired trajectories while avoiding collisions in autonomous flight. A Lyapunov based analysis proved the validity of the closed-loop system despite the presence of external perturbations. Monocular vision is employed to estimate the vehicle's pose of the vehicle and distance to collisions. Real-time experiments are provided.

Keywords: UAVs, Quadrotors, Autonomous Navigation, Sliding Mode, Collision Avoidance, Haptic Teleoperation, Computer Vision.

I. INTRODUCTION

Applications involving flying robots, also known as Unmanned Aerial Vehicles (UAVs), have astonishingly spread out all over the world, in a wide range of tasks where they are used mainly for remote sensing. In particular, four rotor rotorcrafts have attracted special attention from either research groups and industry, thanks to their simplified mechanics and control, and their great maneuverability which allows for vertical take-off and landing, hover, and aggressive flight in small spaces. Such applications include, among others, remote monitoring, surveillance, patrolling, search and rescue, transportation and film recording.

In order to successfully accomplish their mission in an autonomous or semi-autonomous operation, all UAVs require a good estimation of their state vector, with high fidelity and fast rate. Moreover, aerial robots normally present extra challenges steaming from their limited size and payload, constraining their sensing capabilities. Even more, small UAVs are intended to be inexpensive, and the use of high-precision sensing equipment is precluded. Primarily the position, orientation, translational speed and angular rate are needed, hence, they are equipped with a set of sensors normally including an Inertial Measurement Unit (IMU), an optic flow sensor, ultrasound range

[1]Sorbonne universités, Université de technologie de Compiègne, CNRS, Heudiasyc UMR 7253, CS 60 319, 60 203 Compiègne cedex. (dmercado, castillo, rlozano)@hds.utc.fr

[2]LAFMIA UMI 3175 CINVESTAV-CNRS, México.

finders and cameras. A Global Positioning System (GPS) is often used for localization, however, in many scenarios GPS measurements are unavailable, or corrupted due to jamming or environmental constrains.

In fact, localization in GPS-denied environment continues to be an open problem of great interest in the field. Several recent works about this subject can be found in the literature. For example, in [1] the autonomous control problem of a quadrotor in GPS-denied environment is addressed using a miniature laser range finder as the main onboard sensor.

Monocular vision appears as a good option for UAV's perception of their environment, since cameras offer huge amount of information in a compact, lightweight and inexpensive device, at the cost of computational effort. For instance, in [2] a vision-based navigation strategy for UAVs using a single embedded camera observing natural landmarks is presented. Also in [3] the authors proposed a vision-based algorithm to track and land on a known moving target. Vision-based anticipatory controller for the autonomous indoor navigation of an UAV is addressed in [4], where dual feedforward/feedback architecture was used as the UAV's controller and the K-NN classifier using the gray level image histogram as discriminant variables was applied for landmarks recognition. Additionally, in [5] optic flow information from a camera is fused with inertial measurements using an Extended Kalman Filter (EKF) to estimate metric speed, distance to the scene and also acceleration biases.

More in particular, in the last years, some important works to pose estimate using monocular vision have appeared in the literature. They make use of a powerful technique conceived for Augmented Reality (AR) applications, were a hand-held camera is tracked trough a small unstructured workspace. This technique, which is called Parallel Tracking and Mapping (PTAM), is based in the generation of a sparse map composed of thousands of points from the special features on the scene, which can be tracked at frame-rate with high accuracy [6]. In addition, PTAM has been successfully adapted for UAV's localization, by extending the generated map and solving the absolute scale estimation problem using extra information from the quadrotor's embedded sensors. In [7]-[10] the authors introduce implementations of an onboard vision-based UAV controller for navigation on unknown environments without any external assistance. The drawback in these works is to consider expensive aerial prototypes to get a fully embedded system.

Other teams, contrary to the above cited works, have obtained similar results using only a low-cost commercial UAV coupled with a ground-station to compute externally the algorithms [11], [12]. In these research works the system is composed of the PTAM algorithm, an Extended Kalman Filter (EKF) and a linear control. The contribution was to find a solution to the estimation problem for the absolute scale of the generated sparse map, by fusing the visual information with inertial and/or altitude measurements. Furthermore, they provide their complete implementation as open-source code.

On the other hand, obstacle detection and avoidance are key components for the success of autonomous navigation of aerial vehicles. Several teams have explored this matter using different approaches, for example, in [13] the authors proposed a complete system with a multimodal sensor setup for omnidirectional obstacle perception consisting of a 3D laser scanner, two stereo camera pairs, and ultrasonic distance sensors. Detected obstacles were aggregated in egocentric local multiresolution grid maps. Planning of collision-free trajectories and reactive obstacle avoidance were tested in real-time experiments. However, this approach requires a huge payload for the multiple sensors

involved.

Monocular cameras arise again as an excellent alternative to detect and avoid obstacles for small UAVs. First works were based on optical flow algorithms [14] or perspective cues [15], however these methods can not handle frontal obstacles well. In [16], the problem of detecting frontal obstacles for an UAV is examined through a method to detect relative size changes in images patches, with highly confident results in experiments. Similarly, in [17] the authors presented a strategy for a quadrotor with a monocular camera to locally generate collision-free waypoints. In that paper PTAM is used for navigation, then a dense depth map is computed from a small set of images, finally a 2D scan is rendered and suitable waypoints are obtained, but extensive extra computations are required.

In our work, we use the sparse depth map from the special features on the image, provided by the PTAM algorithm, to extend its use to detect possible collisions in the horizontal plane . For a wide range of applications, we consider that no extra computation is needed to generate a dense map for collision avoidance, despite the fact that the sparse map is noisy and weak for low-texture regions. The prototype is a commercial quadcopter Parrot AR.Drone. Collision avoidance is validated in two scenarios; collision free autonomous navigation for trajectory tracking and haptic teleoperation in semi-autonomous mode (only the orientation is in autonomous mode).

High order sliding mode techniques are well-known for their inherent robustness properties with decreasing of the undesired chattering effect typical in sliding mode strategies. Some applications of the sliding mode theory to UAVs can be found in the literature, for example, in [18] the author introduces an attitude controller for mini UAVs using a sliding mode controller and a fuzzy inference mechanism. In [19] a sliding mode fault-tolerant control for an octorotor is proposed, taking advantage on the redundant rotors in this kind of configuration. Also, in [20] a 2-SM is used to achieve attitude control, while position control is addressed using the sliding mode theory in [21], both for quadrotors.

For autonomous navigation, a second order sliding mode controller was designed in this work, to track desired trajectories in a robust way with respect to uncertainties and perturbations, making the closed-loop system suitable for outdoor applications. Such controller is inspired in our previous work [22], but a new term is introduced to include a proportional feedback of the position error, this is intended to improve the closed-loop system's behavior and to help in the parameter tunning. Furthermore, real-time experiments are provided this time to validate the control strategy. Besides, this article is a sequel of our previous work at [23], where the experimental platform was introduced along with some preliminary results for trajectory tracking using a linear control and a feedback linearization, but only for the horizontal plane.

With this control strategy all kinds of mostly translational maneuvers are allowed for trajectory tracking in the $3D$ space. However, since only a frontal camera is used for perception, collision avoidance is only guaranteed for frontal obstacles with enough characteristic points, or previously detected obstacles for lateral motions. In fact, the sparse depth map is projected to the horizontal plane in order to increase the density of points, hence, the algorithm is not able to detect the height of the obstacles, and collision avoidance is not possible along the z axis. This is particularly useful for obstacles like walls and columns.

Our contribution can be summarized in the following points:

- A 3D trajectory tracking control algorithm based on high order sliding mode, robust against perturbations and uncertainties, was proposed and successfully validated in real-time experiments for quadrotors.

- Several tools were assembled and adapted to offer a working solution for either autonomous tracking or semi-autonomous teleoperation. This includes extending the use of the PTAM algorithm to detect and avoid collisions, without extra expensive calculations or sensors.

- In order to improve the safety of the system, without adding any extra sensor, neither requiring expensive calculations, an effective strategy for obstacle avoidance in the horizontal plane was developed.

- Haptic assisted semi-autonomous teleoperation was introduced as an alternative operation mode, taking advantage of the monocular vision based algorithm for collision detection and avoidance.

The rest of this paper is organized as follows: the monocular vision algorithms to pose estimation and the experimental platform are introduced in section II, the proposed 2-SM strategy for robust trajectory tracking with collision avoidance is described in section III. Teleoperation with reactive collision avoidance is addressed in section IV. Main graphs from real time experimental results are presented in section V. Last but not least, section VI states the conclusions and perspectives for future work.

II. EXPERIMENTAL SETUP

A. *Monocular vision localization*

The aerial vehicle position is obtained using computer vision and inertial data fused with an EKF algorithm. The vision algorithm, based on Parallel Tracking and Mapping (PTAM), estimates camera pose in an unstructured scene [6], [9], [11]. The algorithm executes in parallel the vision information for the tracking and mapping. It also constructs a sparse depth map (see Figure 1) which is used in this work to estimate distance to frontal objects.

Even if the PTAM algorithm is a good solution for pose estimation, it was conceived for mostly static and small scenes, and an absolute scale for the map is not provided. This could be considered as a drawback for MAV's (Micro Aerial Vehicles) applications. Nevertheless, in [11] and [12], the authors proposed a nice solution fusing data measurements coming from an IMU, a camera and ultrasounds sensors and using a scale estimator and an EKF. One advantage of this solution is that the vision approach can be obtained as open-source for ROS (Robot Operating System).

For this work, the control algorithm code in [11] was replaced for a new one in order to easily implement and validate different control strategies and help to tune the required gains. Furthermore a trajectory generator was also included for tracking autonomously different kind of time-varying trajectories, rather than just way-points. Finally, the localization algorithm was modified to recover the pointcloud of the depth map generated by the PTAM algorithm, and send it to another node to estimate the distance to potential collisions, as explained in subsection III-B. This way, the operator can select online between the different programed trajectories, control laws and operation modes, as well as modify in real time any parameter for tunning.
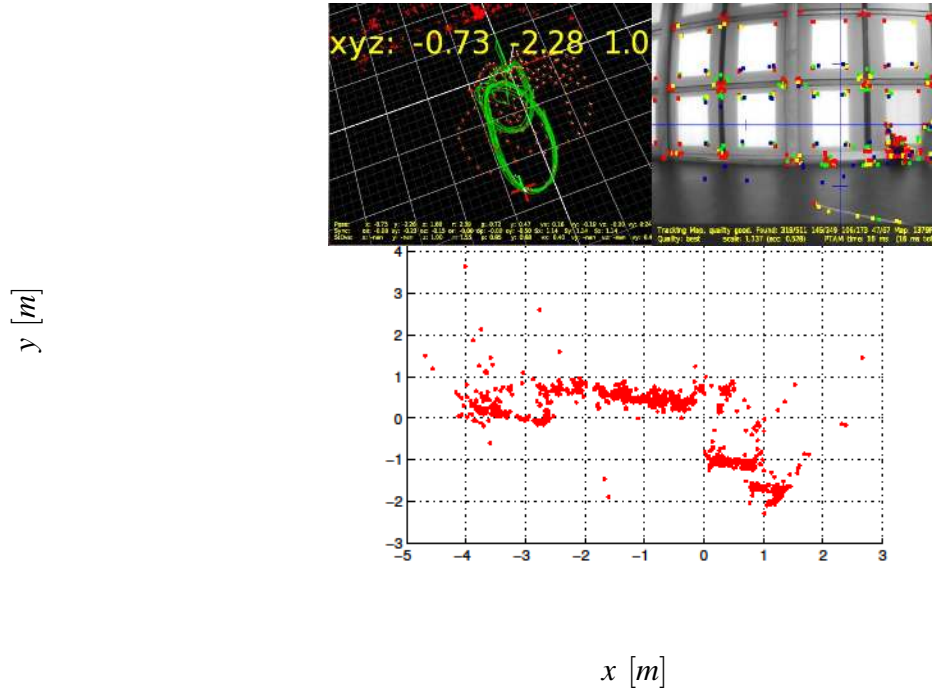
Fig. 1. UAV localization w.r.t. the sparse depth map (top left). Characteristic features on the image (top right). Horizontal projection of the sparse depth map obtained by PTAM (bottom).

B. Prototype

The AR.Drone is a well-known commercial quadrotor (price≈ \$300), which can be used safely close to people and is robust to crashes. It measures 53×52cm and weights 0.42Kg. It is equipped with three-axis gyroscopes and accelerometers, an ultrasound altimeter, an air pressure sensor and a magnetic compass. Also, it provides video streams from two cameras, the first one is looking downwards with a resolution of 320×240 pixels at a rate of 60fps, and is used to estimate the horizontal velocities with an optic flow algorithm. The second camera is looking forward, with a resolution of 640×360 at 30fps, and is used by the monocular vision algorithm.

However, neither the software nor the hardware can be modified easily from the AR.Drone. It includes an internal on-board autopilot to control roll, pitch, altitude velocity and yaw rotational speed (ϕ, θ, $\dot{z}$ and $\dot{\psi}$), according to external references. These references are considered as control inputs and are computed and sent at a frequency of 100 Hz. All sensor measurements are sent to a ground station at a frequency of 200 Hz, where the vision localization and the state estimation algorithms are calculated in real-time on ROS.

C. Haptic Teleoperation

On the other hand, for the haptic teleoperation, the low-cost Novint Falcon haptic device is employed. It consists of a three degrees of freedom haptic interface in a delta configuration, able to feedback forces up to 8.9 N to a

human operator. Its touch workspace is about $10 \times 10 \times 10$ cm, with a resolution larger than 400 *dpi*. An algorithm to connect this haptic device with the vision algorithm was developed in order to improve the flying experience.

III. COLLISION-FREE AUTONOMOUS TRACKING

Let us consider a simplified version of the well-known dynamic model of a quadrotor [24]:

$$m\ddot{\xi} = TRe_3 - mge_3 + w \tag{1}$$

$$\ddot{\Phi} \approx \Gamma \tag{2}$$

with mass m and the gravity constant g. Also, $\xi = [x\ y\ z]^T$ is the position of the quadrotor with respect to an inertial frame, $\Phi = [\phi\ \theta\ \psi]^T$ stands for the Euler angles roll, pitch and yaw. $T \in \Re^+$ defines the total thrust produced by the motors and $\Gamma \in \Re^3$ stands for the control torque produced by the differential of velocities of the rotors. $R \in SO(3)$ represents the rotation matrix from the body fixed frame to the inertial one, and $e_3 = [0\ 0\ 1]^T$. Finally, $w \in \Re^3$ is an external and unknown disturbance vector.

A. 2-Sliding Mode Trajectory Tracking Control

Time-scale separation allows us to hierarchically design separate controllers for the rotational and translational dynamics [25]. This is possible since the close loop rotational subsystem is much faster than the translational one, hence, desired references for the attitude are used as virtual control inputs for the trajectory tracking control of the position. Note that this is suitable for most commercial available UAVs with internal autopilot.

Then, the control objective is to design a trajectory tracking control for autonomous navigation in outdoor flight, using orientation references as virtual control inputs. Therefore, some robustness is required to deal with external perturbation and uncertainties produced by the changing weather conditions, mainly the wind. A second order sliding mode was selected for this issue, thanks to its well-known robustness property against perturbations and uncertainties [26].

Define the desired position ξ_d and the position error as $\bar{\xi} = \xi - \xi_d$, then substituting into (1) leads to

$$m\ddot{\bar{\xi}} = (TRe_3)_d - mge_3 - m\ddot{\xi}_d + w \tag{3}$$

Let us consider the so called switching function with relative degree 2

$$\sigma = \dot{\bar{\xi}} + k_1 \int \bar{\xi}\, dt \tag{4}$$

where $k_1 \in \Re^{3x3}$ is a diagonal positive definite gain matrix. Then calculating the second time derivative

$$\dot{\sigma} = \ddot{\bar{\xi}} + k_1\dot{\bar{\xi}} = \frac{1}{m}(TRe_3)_d - ge_3 - \ddot{\xi}_d + k_1\dot{\bar{\xi}} + \frac{w}{m} \tag{5}$$

Consider now $u = (TRe_3)_d$ to be the control input. Then using the Twisting Algorithm [26], the following discontinuous controller is proposed

$$u = m(ge_3 + \ddot{\xi}_d - k_1\dot{\bar{\xi}} - r_1 Sgn(\sigma) - r_2 Sgn(\dot{\sigma}) - k_2\dot{\sigma}) \tag{6}$$

where the first three terms will annihilate the continuous dynamics of the closed loop system, while the next two expressions introduce the discontinuous control. Note the inclusion of the final term $(-k_2\dot{\sigma})$, which induces a proportional feedback of the position error, it is aimed to improve the controller behavior and facilitate the parameters tunning. r_1, r_2, $k_2 \in \Re^+$ are constant control parameters.

Here, a vectorial sign function is employed, then for a vector $\Upsilon = [v_1\ v_2\ v_3]^T$ we will have

$$
Sgn(\Upsilon) = \begin{bmatrix} sgn(v_1) \\ sgn(v_2) \\ sgn(v_3) \end{bmatrix} ; \quad sgn(v_i) = \begin{cases} 1 & v_i > 0 \\ 0 & v_i \in [-1,1] \\ -1 & v_i < 0 \end{cases}
\tag{7}
$$

Then, using a suitable variation of the Lyapunov stability theory for non-smooth Lipschitz continuous Lyapunov functions [27], we can analyze the stability of the control system. Let us consider the following Lipschitz continuous Lyapunov function

$$
V = r_1 ||\sigma||_1 + \frac{1}{2}\dot{\sigma}^T\dot{\sigma}
\tag{8}
$$

differentiating (8) with respect to time, everywhere but on $\sigma = 0$ where V is not differentiable, leads to

$$
\dot{V} = r_1 Sgn(\sigma)^T\dot{\sigma} + \ddot{\sigma}^T\dot{\sigma}
\tag{9}
$$

and after some manipulations

$$
\dot{V} \leq ||\dot{\sigma}||_1 (-r_2 + \frac{1}{m}||w||) - k_2\dot{\sigma}^2
\tag{10}
$$

if the external disturbance is bounded $||w|| \leq ma$, for some $a > 0$, and choosing $r_2 > a$ we have $\dot{V} \leq 0$.

Applying an extended version of the LaSalle invariant principle [27], and following a similar procedure as the one presented in [22], we can show that choosing $r_1 > r_2 + a$, the largest invariant set where $\dot{V} = 0$ contains only the origin $\sigma = \dot{\sigma} = 0$, and all the trajectories of the system converge to zero.

It is important to notice that

$$
R_d e_3 = \begin{bmatrix} R_{dx} \\ R_{dy} \\ R_{dz} \end{bmatrix} = \frac{(TRe_3)_d}{T_d}
\tag{11}
$$

with $T_d = ||(TRe_3)_d||$.

Proposing a constant ψ_d, and using the short notation $s\alpha = \sin(\alpha)$, $c\alpha = \cos(\alpha)$, it is possible to find ϕ_d and θ_d explicitly as

$$
\phi_d = \arcsin\left(R_{dx}s\psi_d - R_{dy}c\psi_d\right)
\tag{12}
$$

$$
\theta_d = \arcsin\left(\frac{R_{dx}c\psi_d + R_{dy}s\psi_d}{c\phi_d}\right)
\tag{13}
$$

where ϕ_d and θ_d are the desired roll and pitch angles provided to the AR.Drone.

B. Collision Avoidance

One of the main challenges in autonomous navigation for mobile robots such as UAVs, is the perception of unknown environments, with the extra difficulty of the limited payload. In the present work, we are interested in detecting possible collisions using the already available information from the sensors of an inexpensive commercial quadrotor. Particularly we are interested in using monocular vision with the frontal camera to estimate the distance to obstacles by taking advantage of the sparse depth map generated by the localization algorithm.

Then, distance to possible collisions is estimated from the horizontal projection of the sparse depth map computed by the PTAM algorithm, as the one showed in Figure 1. It consists of a set P of n points $p_i(x_i, y_i, z_i)$, $i = 1, .., n$ obtained from the characteristic features of the image stream provided by the frontal camera of the quadrotor. PTAM uses these points as a map to estimate the pose of the UAV. An horizontal projection of this point cloud is used in this work, i.e., all the obstacles are considered to have the same height (this stands for walls, columns, etc.). However, it results in a very noisy depth map and should be given special care for obstacles presenting low-texture surfaces for the vision algorithm.

Therefore, we define the estimated distance to frontal obstacles d_y as

$$d_y = y - \frac{1}{\eta_y} \sum_{i \in \Omega_y} y_i$$

$$\Omega_y = \{p_i(x_i, y_i, z_i) \in P \mid x_i \in [x - \varepsilon, x + \varepsilon]\}$$

(14)

i. e., the average depth, w.r.t. the position of the quadrotor along y, of the η points inside certain lateral range ε from the lateral position of the quadrotor x. Analogously, we can obtain the estimated distance to lateral obstacles d_x.

In order to avoid collisions, we apply a potential field, such that if distance d_i ($i = x$, y) falls bellow certain safe distance d_s, then, a repulsive force F_{rep_i} will be exerted as follows

$$F_{rep_i} = \begin{cases} 0 & \left| \begin{array}{l} d_i > d_s \end{array} \right. \\ -k_{rep_i}(\frac{1}{d_i} - \frac{1}{d_s})(\frac{1}{d_i^2}) & \left| \begin{array}{l} d_i \leq d_s \end{array} \right. \end{cases}$$

(15)

Finally, retaking the 2-SM trajectory tracking control (12) and (13), the full collision-free trajectory tracking strategy becomes

$$\phi_d = \arcsin\left(R_{dx}s\psi_d - R_{dy}c\psi_d\right) + F_{rep_y}$$

(16)

$$\theta_d = \arcsin\left(\frac{R_{dx}c\psi_d + R_{dy}s\psi_d}{c\phi_d}\right) + F_{rep_x}$$

(17)

It must be noted that lateral obstacle detection becomes much more challenging, since only a frontal camera is used for this purpose.

IV. HAPTIC TELEOPERATION

Although huge advances have been accomplished in the research for fully autonomous UAVs, human tele-operated UAVs remain as a good alternative due to the still unsolved issues and security constrains related to the fully autonomous ones. Still, it is important to aid the operator with his tasks as much as possible, by providing

him useful information and making the operation more intuitive. Even more, it is necessary to minimize the risk of human mistakes.

Haptic devices appear as a good option to assist humans in the teleoperation of systems such as UAVs. Haptic is tactile feedback technology which recreates the sense of touch by applying forces, vibrations, or motions to the user. In this sense, haptic technologies can be applied to UAVs teleoperation in order to improve the pilot's experience by providing him feedback of forces. For example, he would be able to feel a gust of wind or any other external perturbation affecting the vehicle. It can also be used to prevent the user from executing forbidden or risky actions such as driving the UAV to unsafe areas or out of the range of communication.

In this work, we are interested in investigating the use of haptic devices for safe UAV teleoperation by preventing the user to crash the quadrotor against potential obstacles. The most common techniques for haptic feedback to avoid collisions in UAVs are force feedback (for example artificial force field), and stiffness feedback using a virtual spring. A comparative analysis of these techniques can be found in [28] and [29].

In this paper we successfully applied the Novint Falcon haptic device to assist in teleoperation and prevent the user from crashing the quadrotor against an obstacle. To do so, the position of the final effector of the haptic device (x_h, y_h, z_h) provides in a linear relation the desired roll and pitch angles (ϕ_d, θ_d) and the desired altitude velocity $(\dot{z}_d)$, respectively. It is

$$\phi_d = k_{hy}(y_h - o_y)$$
$$\theta_d = k_{hx}(x_h - o_x) \quad (18)$$
$$\dot{z}_h = k_{hz}(z_h - o_z)$$

where k_{hx}, k_{hy}, k_{hz}, o_x, o_y, o_z are suitable gains and offsets. This strategy is useful for quadrotors with an internal orientation and altitude controllers. Observe from (18) that to keep the quadrotor hovering in a desired position, the user should keep the haptic device at the center of its workspace. In order to assist the user in this task, and simplify the manual control of the UAV, a proportional derivative controller is applied to regulate the haptic's final effector position at the origin if no force from the operator is exerted. Similarly, a repulsive force is applied to the haptic device once the quadrotor approaches an obstacle. Then, the feedback forces applied to the haptic device are defined as

$$F_x = \begin{cases} -k_{phx}x - k_{dhx}\dot{x} & d_x > d_s \\ -k_{hrep_x}(\frac{1}{d_x} - \frac{1}{d_s})(\frac{1}{d_x^2}) & d_x \leq d_s \end{cases}$$
$$F_y = \begin{cases} -k_{phy}y - k_{dhy}\dot{y} & d_y > d_s \\ -k_{hrep_y}(\frac{1}{d_y} - \frac{1}{d_s})(\frac{1}{d_y^2}) & d_y \leq d_s \end{cases} \quad (19)$$
$$F_z = -k_{phz}z - k_{dhz}\dot{z}$$

with the control gains k_{phx}, k_{phy}, k_{phz}, k_{dhx}, k_{dhy}, k_{dhz}, $k_{hrep_i} \in \Re^+$.

V. REAL TIME EXPERIMENTS

Extensive experiments were executed to validate the proposed algorithms. The practical validations were developed in three ways; autonomous trajectory tracking close to a wall, surround a column-kind obstacle and haptic

teleoperation. The parameters used for the first an third cases were tuned by trial and error and are presented in Table I. For surrounding a column, the gains were relaxed due to the difficulty of the problem while dealing with a lateral obstacle and using only a frontal camera for detection.

TABLE I

PARAMETERS

k_1	k_2	$\varepsilon[m]$	k_{rep}	$d_s[m]$	
2	25	0.5	4	5	
k_{hx}	k_{hy}	k_{hz}	$k_{phx,y,z}$	$k_{dhx,y,z}$	$k_{hrep_{x,y}}$
12.7	14.3	18.2	100	500	2
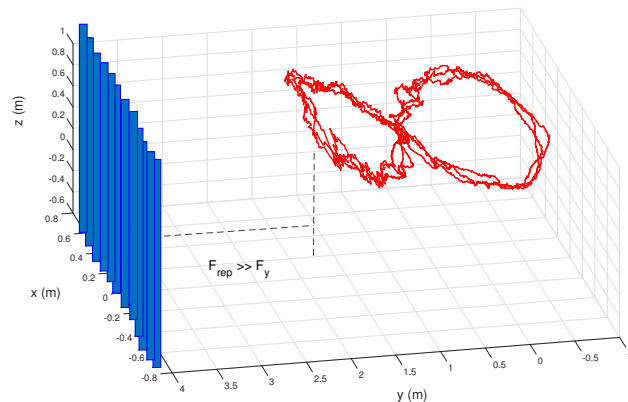
Fig. 2. 3D Collision-free lemniscate trajectory tracking close to a wall.

Some experiments can be found on video at https://www.youtube.com/watch?v=bb7ooBvcHHk.

A. Trajectory tracking

In this test, the mission was to follow autonomously a lemniscate trajectory with a length of 3m. The challenge in this mission is to introduce a wall close to the trajectory, such that the vehicle, using the monocular camera detects the wall and activates the repulsive algorithm for collision avoidance.

Figure 2 illustrates the experiment in a 3D view, where we can appreciate how the vehicle modifies its trajectory when it is close to the wall, see also Figure 3. Notice here that the repulsive force F_{rep} becomes bigger than the force generated by the tracking control F_y while approaching the wall, producing the deflection with respect to the
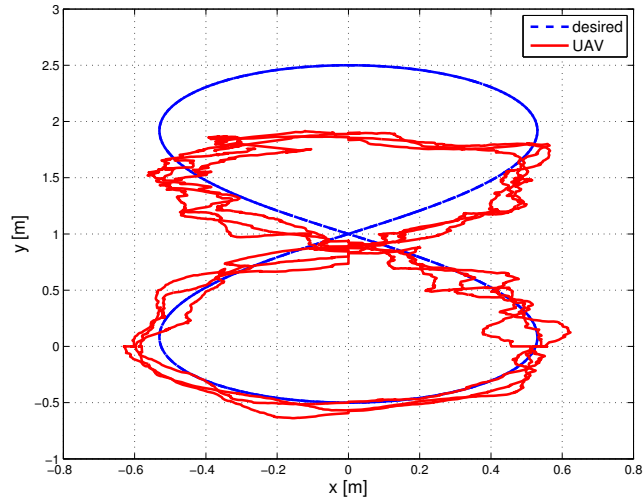
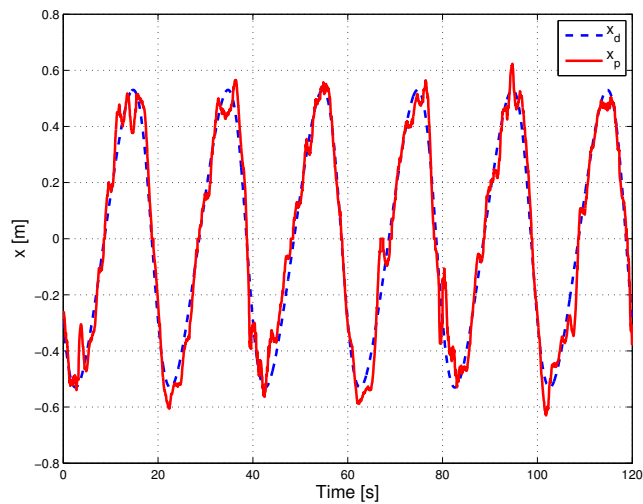Fig. 3. Collision-free trajectory tracking.

Fig. 4. x position response for a lemniscate trajectory.

desired trajectory. This is expected since the safety of the system is more important than accomplishing the tracking mission. The aerial view of this result is illustrated in Figure 3.

Figures 4 and 5 show the x and y states of the quadrotor while following the trajectory close to a wall. Observe in these figures that the quadrotor carries out very well the path tracking in the y coordinate, except when the quadrotor approaches the wall and the repulsive force acts on the control scheme, see Fig. 5. Meanwhile in the x position, see Fig. 4, some minor error can be observed due to the more aggressive nature of the lemniscate trajectory on this axis.
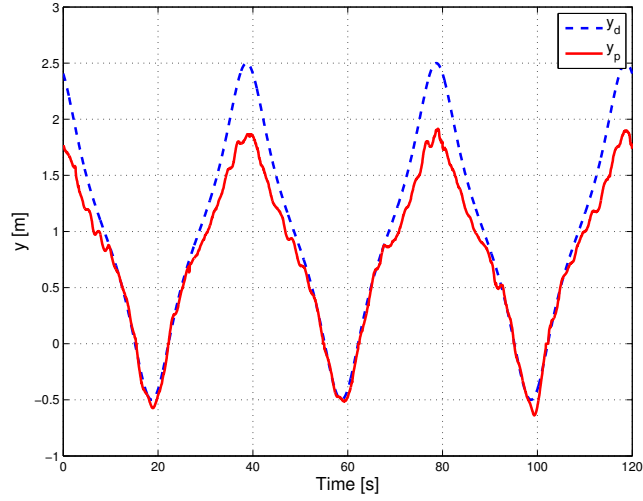
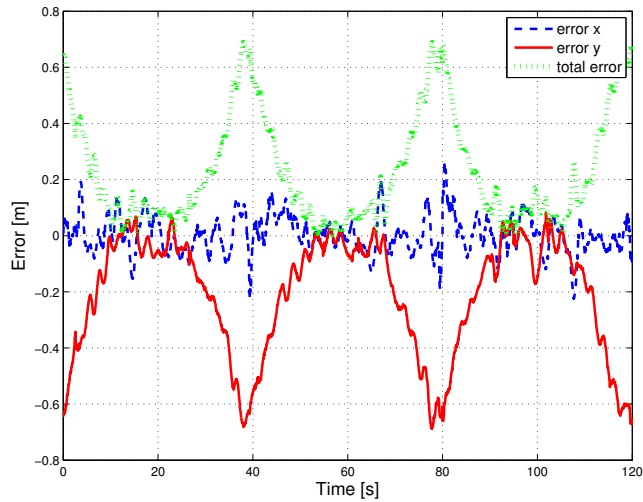Fig. 5. *y* position response for a lemniscate trajectory.

Fig. 6. Tracking errors.

In Figure 6 the tracking errors $\bar{\xi}_x$, $\bar{\xi}_y$ are displayed, along with the total error $\sqrt{\bar{\xi}_x^2 + \bar{\xi}_y^2}$. These errors always remain bounded in small values except for the time when the UAV get close to the wall. The control inputs for the internal autopilot are depicted in Figure 7. It is important to point out that small gains have been chosen in the discontinuous terms, for the real time implementation to avoid aggressive commands. This is due to the discontinuous nature of the controller, to solve this issue, it is considered to explore in future developments a super-twisting algorithm, to attenuate the undesired chattering effect.

From this experiment we can conclude that the trajectory tracking control performs well when no obstacle is
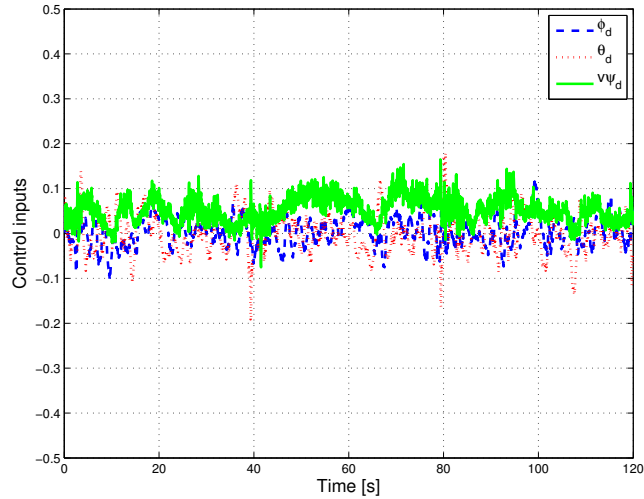
Fig. 7. Trajectory tracking control inputs.

present. Meanwhile, obstacle avoidance is possible using only a frontal camera for detection and without any extra expensive computation, for obstacles like flat walls. In order to test the collision avoidance strategy in a more challenging scenario, the following section address the problem of surrounding a column to arrive to a desired position.

B. Surrounding an obstacle

Fig. 8. Obstacle avoidance.

In this case, the objective consists in going from point (0,0) to (0,9) without clashing against the obstacle localized halfway, as depicted in Figure 9. Such obstacle of irregular shape is unknown for the UAV, who must detect it and surround it in order to accomplish its mission without collision (see Fig. 8).
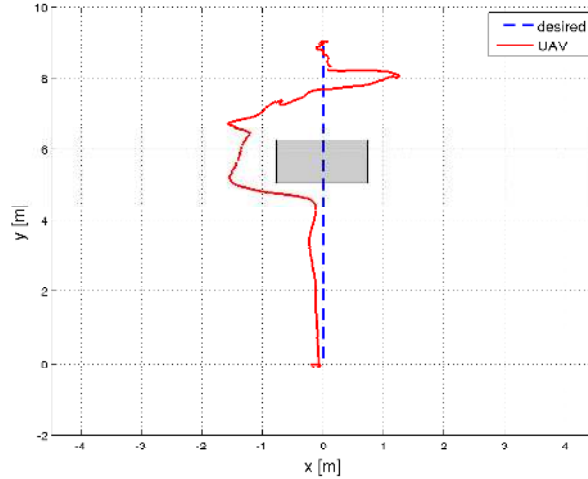
Fig. 9. Quadrotor surrounding an obstacle.

The experimental results are presented in Figures 9 to 12. In Fig. 9 we can appreciate the performed trajectory by the UAV in the horizontal plane. We can see how the quadrotor was able to detect the obstacle and change its course to continue its mission without collision. Hence, a frontal repulsive force is exerted to prevent the UAV from colliding, and once the UAV is close to the obstacle, a lateral repulsive force allows to evade the obstacle and continue to the goal. Figures 10 and 11 corroborate this for each coordinate x and y. From the x position in Fig. 10, we can observe that there is a big overshoot at second 22, once the quadrotor passes the obstacle and tries to retake its way to the goal. This is probably due to a poor gain adjustment in the x coordinate. Meanwhile, on Fig. 11 we can appreciate how the helicopter converges to the reference almost exponentially, despite the presence of the obstacle.
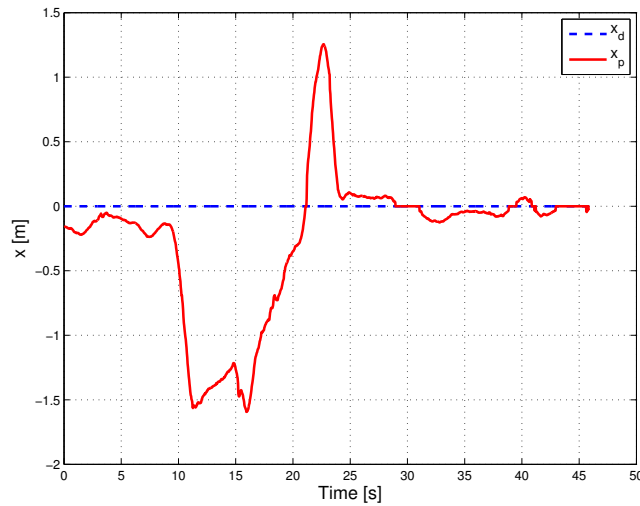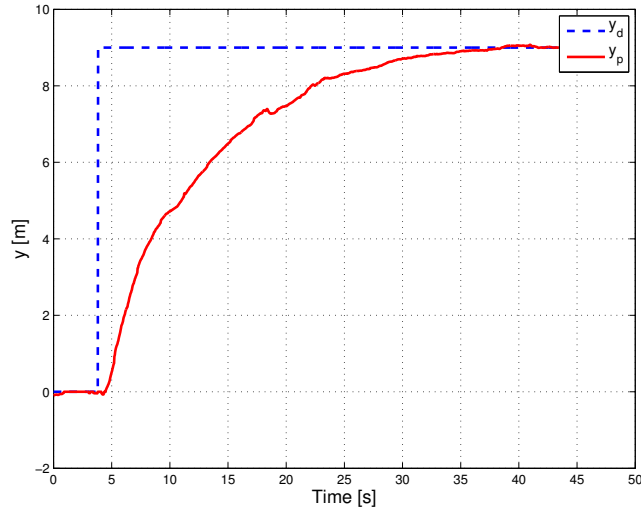

Fig. 10. x coordinate.

Fig. 11. *y* coordinate.

Finally, Fig. 12 shows the quadrotor's orientation while performing the task. It is interesting to note the attitude maneuvers performed by the UAV in order to quickly go to the target in second 4, and in order to evade the obstacle in second 9. We can also observe some peaks at seconds 15 and 21 probably due to noise in the point cloud.
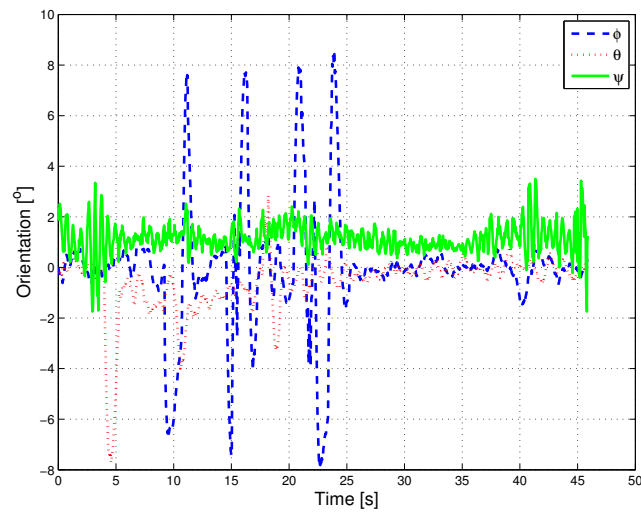

Fig. 12. Attitude.

C. Collision free teleoperation

For the teleoperation scenario, a human pilot controls the position of the quadrotor through a haptic device. The practical goal here is to use the haptic device to feedback information from the vehicle to the pilot and prevent him from colliding, via opposite forces in the haptic device when the quadrotor goes out of a safety zone. This is useful, for example, in wall-inspection missions were the operator's visibility is limited.
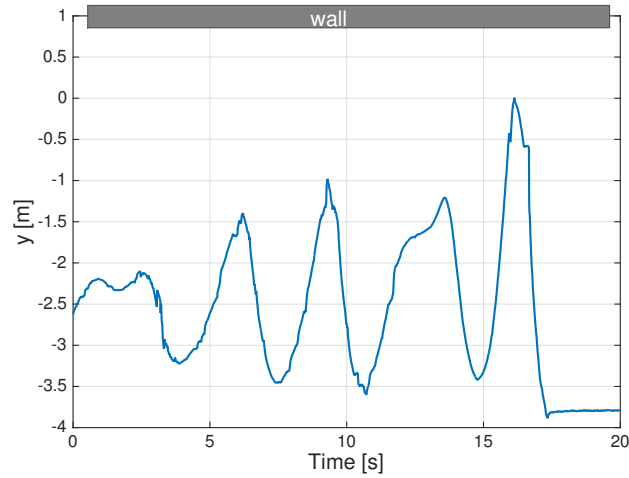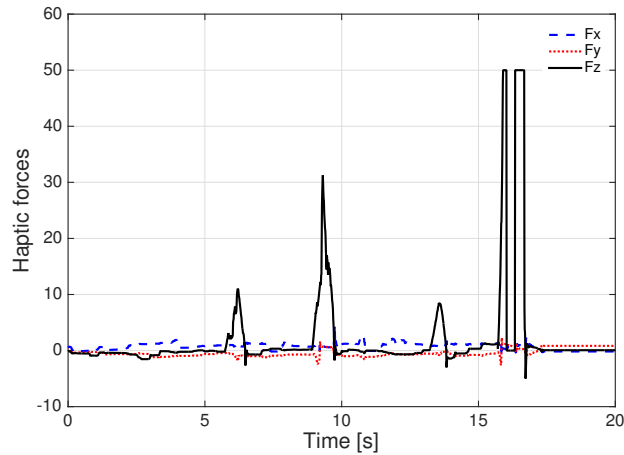
Fig. 13. y coordinate.

Fig. 14. Haptic feedback forces.

Collision free haptic teleoperation is studied through Figures 13-15. In these flight tests, the user flew the UAV in semi-autonomous mode using a haptic device. Here, only the orientation is in autonomous mode. The user attempts to crash deliberately the vehicle against a frontal wall, a few times. The first tries were realized slowly, but the last was done at high speed.

The position response in the y state of the UAV through the experiments is depicted in Figure 13, observe in this figure at times $6s$, $9s$ and $13.5s$, how the reactive collision avoidance algorithm prevented the user from driving the quadrotor to a dangerous area too close to the wall. Furthermore, at time $16s$ the pilot deliberately tried to crash the UAV in a fast maneuver toward the wall, even thought it get to touch the wall, it never crashes thanks to the good performance of the proposed algorithm even in this extreme case. Finally, observe in Figures 14 and 15 the feedback force applied to the haptic device and the control inputs send to the UAV, respectively. When approaching
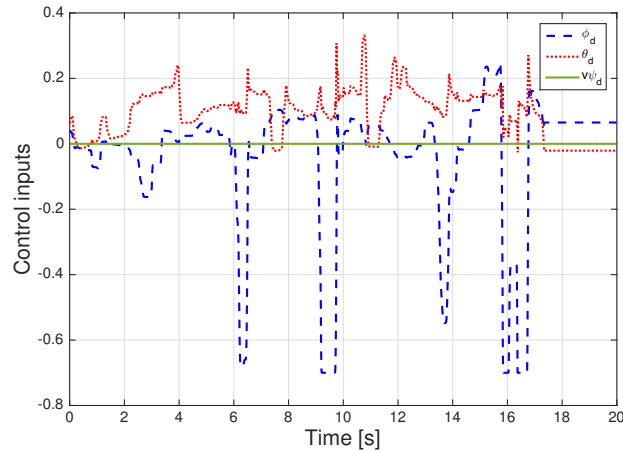
Fig. 15. UAV control inputs.

the wall, the haptic device exerts a repulsive force alerting the human operator of the danger and even forbidding him from crashing the quadrotor, see second 16 on Figures 14 and 15.

It is important to point out that the obtained results are quite satisfactory, taking into account that only a monocular camera is used to locate the quadrotor and to detect collisions, instead of using an expensive motion capture system and/or extra range sensors as others teams. Henceforth, the obtained results can be easily reproduced on outdoor flight tests.

VI. CONCLUSION & FUTURE WORK

Collision-free navigation and teleoperation for a quadrotor using only a monocular camera were presented and experimentally validated in this article. Two main cases were studied: autonomous collision-free trajectory tracking and collision-free teleoperation. Despite the simplicity of the proposed collision avoidance technique, it satisfactorily accomplished its goal for both studied cases.

Second order sliding mode control proved to be adequate for accurate trajectory tracking with the presented setup, accomplishing well the tracking objective while adding robustness against external perturbations. However, special attention must be payed when implementing this kind of controllers because of their discontinuous nature, in this case, the discontinuous terms were kept bounded by choosing small gains. It is desired to test a second order sliding mode control using the super-twisting algorithm to attenuate the chattering effect.

Haptic assisted teleoperation has been demonstrated to be an interesting alternative for safe UAV navigation, preventing the user from colliding the UAV and improving the flying experience. Monocular-vision based navigation showed to be a powerful tool for MAV's in GPS denied environments, as well as an exciting research area to be explored.

Future work includes to extend the obtained results for outdoor tests, and to improve the obstacle detection for the lateral direction by adding extra sensors or using more sophisticated techniques for point-cloud filtering.

REFERENCES

[1] Y. Song, B. Xian, Y. Zhang, X. Jiang and X. Zhang. "Towards Autonomous Control of Quadrotor Unmanned Aerial Vehicles in a GPS-denied Urban Area via Laser Ranger Finder". In *Optik*, 2015.

[2] J. Courbon, Y. Mezouar, N. Guenard and P. Martinet. "Vision-based Navigation of Unmanned Aerial Vehicles". In *Control Engineering Practice*, 2010.

[3] Y. Bi and H. Duan. "Implementation of Autonomous Visual Tracking and Landing for a Low-cost Quadrotor". In *Optik*, 2013.

[4] D. Maravall, J. de Lope, J. Fuentes. "Vision-based Anticipatory Controller for the Autonomous Navigation of an UAV using Artificial Neural Networks". In *Neurocomputing*, 2015.

[5] P. Li, M. Garratt, A. Lambert and S. Lin. "Metric Sensing and Control of a Quadrotor using a Homography-based Visual Inertial Fusion Method". In *Robotics and Autonomous Systems*, 2016.

[6] G. Klein and D. Murray. "Parallel Tracking and Mapping for Small AR Workspaces". In *Proc. IEEE Intl. Symposium on Mixed and Augmented Reality (ISMAR)*, 2007.

[7] M. Achtelik, M. Achtelik, S. Weiss and R. Siegwart. "Onboard IMU and Monocular Vision Based Control for MAVs in Unknown In- and Outdoor Environments". In *Proc. of the IEEE International Conference on Robotics and Automation (ICRA)*, 2011.

[8] S. Weiss, M. Achtelik, S. Lynen, M. Chli and R. Siegwart. "Real-time Onboard Visual-Inertial State Estimation and Self-Calibration of MAVs in Unknown Environments". In *Proc. of the IEEE International Conference on Robotics and Automation (ICRA)*, 2012.

[9] S. Weiss, D. Scaramuzza and R. Siegwart. "Monocular-SLAM-Based navigation for autonomous micro helicopters in GPS-denied environments". In *Journal of Field Robotics*, Vol. 28, No. 6, 854-874, 2011.

[10] S. Weiss, S., M. Achtelik, S. Lynen, M. Achtelik, L. Kneip, M. Chli, & Siegwart, R. "Monocular Vision for Long-term Micro Aerial Vehicle State Estimation: A Compendium". In *Journal of Field Robotics*, Vol. 30, no. 5, 2013.

[11] J. Engel, J. Sturm and D. Cremers. "Camera-Based Navigation of a Low-cost Quadrocopter". In *Proc. IEEE Intl. Conf. on Intelligent Robot Systems (IROS)*, 2002.

[12] J. Engel, J. Sturm and D. Cremers. "Scale-Aware Navigation of a Low-Cost Quadrocopter with a Monocular Camera". In *Robotics and Autonomous Systems*, vol. 62, issue 11, pp. 1646-1656, 2014.

[13] M. Nieuwenhuisen, D. Droeschel, M. Beul and S. Behnke. "Obstacle Detection and Navigation Planning for Autonomous Micro Aerial Vehicles". In *Proceedings of International Conference on Unmanned Aircraft Systems (ICUAS)*, 2014.

[14] A. Beyeler, J. Zufferey, and D. Floreano, "3D Vision-based Navigation for Indoor Microflyers". In *Proceedings IEEE International Conference on Robotics and Automation (ICRA)*, 2007.

[15] C. Bills, J. Chen, and A. Saxena. "Autonomous MAV flight in indoor environments using single image perspective cues". In *IEEE International Conference on Robotics and Automation (ICRA)*, 2011.

[16] T. Mori and S. Scherer. "First Results in Detecting and Avoiding Frontal Obstacles from a Monocular Camera for Micro Aerial Vehicles". In *IEEE International Conference on Robotics and Automation (ICRA)*, 2013.

[17] H. Alvarez, L. M. Paz, J. Sturm and D. Cremers. "Collision Avoidance for Quadrotors with a Monocular Camera". In *Proc. of The 12th International Symposium on Experimental Robotics (ISER)*, 2014.

[18] F. Yeh. "Attitude controller design of mini-unmanned aerial vehicles using fuzzy sliding-mode control degraded by white noise interference". In *IET Control Theory and Applications*, Vol. 6, Iss. 9, pp. 12051212 1205, 2012.

[19] H. Alwi and C. Edwards. "Sliding mode fault-tolerant control of an octorotor using linear parameter varying-based schemes". In *IET Control Theory and Applications*, Vol. 9, Iss. 4, pp. 618636, 2015.

[20] L. Derafa, L. Fridman, A. Benallegue & Ouldali. "Super Twisting Control Algorithm for the Four Rotors Helicopter Attitude Tracking Problem". *In 11th International Workshop on Variable Structure Systems*, Mexico City, Mexico, 2010.

[21] R. Xu & Ü. Özgüner. "Sliding mode control of a quadrotor helicopter". *In Proc. 45th IEEE Conference on Decision & Control*, 2006.

[22] D. Mercado, P. Castillo, R. Castro and R. Lozano. "2-Sliding Mode Trajectory Tracking Control and EKF Estimation for Quadrotors". *In the 19th IFAC World Conference*, Cape Town, South Africa, 2014,

[23] D. Mercado, P. Castillo and R. Lozano. "Quadrotor's Trajectory Tracking Control using Monocular Vision Navigation". *In International Conference on Unmanned Aircraft Systems (ICUAS)*, Denver, USA, 2015.

[24] P. Castillo, R. Lozano A. Dzul. "Modelling and control of mini-flying machines". *Springer-Verlag*, Londres, 2005.

[25] S. Bertrand, N. Gunard, T. Hamel, H. Piet-Lahanier & L. Eck. "A hierachical controller for miniature VTOL UAVs: Desing and stability analysis using singular perturbation theory". In *Control Engineering Practice*, 19, 1099-1108. 2011.

[26] Y. Shtessel, C. Edwards, L. Fridman & A. Levant. "Sliding Mode Control and Observation", *B*irkhauser, 2010.

[27] D. Shevitz and B. Paden. "Lyapunov stability theory of nonsmooth systems". In *In IEEE Trans. Automat. Control* 39, pp. 1910-1914, 1994.

[28] T. Lam, M. Mulder and M. van Paasen. "Haptic Feedback for UAV Tele-operation - Force offset and spring load modification". In *IEEE International Conference on Systems, Man, and Cybernetics*, 2006.

[29] A. Brandt and M. Colton. "Haptic Collision Avoidance for a Remotely Operated Quadrotor UAV in Indoor Environments". In *IEEE International Conference on Systems, Man, and Cybernetics*, 2010.